Available online at www.sciencedirect.com

SCIENCE DIRECT®

Tectonophysics 385 (2004) 105–120

TECTONOPHYSICS

www.elsevier.com/locate/tecto

Seismogenic structures along continental convergent zones: from oblique subduction to mature collision

Wang-Ping Chen*, Chu-Yung Chen

Department of Geology, University of Illinois at Urbana-Champaign, Urbana, IL 61801, USA

Accepted 26 April 2004
Available online 24 June 2004

Abstract

We summarize seismogenic structures in four regions of active convergence, each at a different stage of the collision process, with particular emphases on unusual, deep-seated seismogenic zones that were recently discovered. Along the eastern Hellenic arc near Crete, an additional seismogenic zone seems to occur below the seismogenic portion of the interplate thrust zone—a configuration found in several other oblique subduction zones that terminate laterally against collision belts. The unusual earthquakes show lateral compression, probably reflecting convergence between the subducting lithosphere's flank and the collision zone nearby. Along oblique zones of recent collision, the equivalence between space and time reveals the transition from subduction to full collision. In particular, intense seismicity beneath western Taiwan indicates that along the incipient zone of arc–continent collision, major earthquakes occur along high-angle reverse faults that reach deep into the crust or even the uppermost mantle. The seismogenic structures are likely to be reactivated normal faults on the passive continental margin of southeastern China. Since high-angle faults are ineffective in accommodating horizontal motion, it is not surprising that in the developed portion of the central Taiwan orogen (< 5 Ma), seismogenic faulting occurs mainly along moderate-dipping (20–30°) thrusts. This is probably the only well-documented case of concurrent earthquake faulting on two major thrust faults, with the second seismogenic zone reaching down to depths of 30 km. Furthermore, the dual thrusts are out-of-sequence, being active in the hinterland of the deformation front. Along the mature Himalayan collision zone, where collision initiated about 50 Ma ago, current data are insufficient to distinguish whether most earthquakes occurred along multiple, out-of-sequence thrusts or along a major ramp thrust. Intriguingly, a very active seismic zone, including a large ($M_w = 6.7$) earthquake in 1988, occurs at depths near 50 km beneath the foreland. Such a configuration may indicate the onset of a crustal nappe, involving the entire cratonic crust. In all cases of collision discussed here, the basal decollement, a key feature in the critical taper model of mountain building, appears to be aseismic. It seems that right at the onset of collision, earthquakes reflect reactivation of high-angle faults. For mature collision belts, earthquake faulting on moderate-dipping thrust accommodates a significant portion of convergence—a process involving the bulk of crust and possibly the uppermost mantle.

Keywords: Earthquakes; Active tectonics; Mountain building; Orogeny

* Corresponding author.
E-mail address: wpchen@uiuc.edu (W.-P. Chen).

0040-1951/$ - see front matter © 2004 Elsevier B.V. All rights reserved.
doi:10.1016/j.tecto.2004.04.022

1. Introduction

In late 1999, several damaging earthquake sequences occurred in Turkey and Taiwan. The devastation caused by these events once again underscores the importance of understanding seismogenic (earthquake generating) structures—a critical first step in the evaluation and mitigation of seismic hazard.

While the Izmit and the Duzce sequences in Turkey occurred along a well-known seismogenic structure, the northern Anatolian fault system (e.g., Toksoz, 2002); the Chi-Chi sequence of September 20, 1999 in Taiwan was a surprise in several respects. First, background seismicity has been low in the source zone since data from modern instrumentation became available in the early 1970s (Shin et al., 2000). Second, the magnitude of the Chi-Chi main shock (~ 7.5) far exceeds the moderate range of estimated magnitudes (5.5–6.8) for historical earthquakes in central Taiwan (Cheng et al., 1999). Third, detailed analysis of source mechanisms of the sequence revealed concurrent slip on out of sequence thrusts that dip at moderate angles ($\sim 25°$) and reach down to depths near 30 km (Kao and Chen, 2000; Chen and Kao, 2000a). This type of seismogenic faulting is a new finding, never well-documented elsewhere.

Indeed the advent of broadband (high-resolution), digital seismometry in the late 1980s has provided a powerful tool of unprecedented resolution to illuminate seismogenic structures whose great depth makes them inaccessible to most other means of investigation. In this paper, we summarize four cases whereby high-resolution earthquake data exposed unusual seismogenic structures along different zones of continental convergence: eastern Hellenic trench, southwestern Taiwan, central Taiwan, and central Himalayas–southern Tibet. Since each case appears to be unique and since each region appears to be at a particular stage of tectonic evolution, we take the position that a region's maturity along its temporal path of tectonic evolution is an important factor in the development of seismogenic structures.

On one hand, this is partially a review paper in that with the exception of results for the southwestern Taiwan orogen, most earthquake data and analysis appeared in the literature elsewhere. On the other hand, except for the Chi-Chi sequence in central Taiwan, we present new syntheses and holistic interpretations that are based on precisely determined focal depths and fault plane solutions of the dense, recent seismicity, geologic mapping, seismic reflection profiles, geodesy, and drilling. Such an approach results in the identification of deep-seated seismogenic structures that received only sparse attention in the past. In particular, seismic faulting is often thick-skinned, involving the bulk of crust and possibly the uppermost mantle.

2. Analysis and regional synthesis of data

For seismogenic structures, we take care to include only reliable results of high-resolution. In general, there are two major sources of data. In the first category, results come from the inversion of broadband waveforms recorded at local and regional distances (up to epicentral distances, Δ, of about 10°). Data from close-in stations lead to precise locations of epicenters, and the inclusion of many small earthquakes provides broad spatial coverage for structures of interest. Conversely, complexity due to wave propagation often forces the use of only low-frequency waveforms, thus reducing the spatial resolution of results. Moreover, so far few sets of regional broadband waveforms are available for important earthquake sequences.

In the second category, results are from the inversion of broadband waveforms of *P*- and *S*-waves recorded at teleseismic distances ($\Delta \sim 30-90°$). This approach complements the inversion of local/regional waveforms. In particular, one can easily account for most effects due to wave propagation, resulting in highly precise focal depths and fault plane solutions (e.g., Nábelek, 1984). In addition, there is little restriction in geographic coverage and all data are in the public domain. A major limitation, however, is that only moderate-to large earthquakes ($m_b \geq 5.5$) generate waveforms of sufficiently high signal-to-noise ratio for the inversion, reducing the number of earthquakes available for study.

In this paper, we take advantage of a fortuitous situation in Taiwan where data from both regional and teleseismic distances are available for many large earthquakes since 1995. As such, results from

regional waveforms are calibrated against those from teleseismc data (Kao and Chen, 2000). This procedure ensures a uniform resolution to elucidate seismogenic structures discussed in this paper.

For each region, we synthesize a variety of data, including those from geologic mapping, modern geodesy (using GPS), seismic reflection profiles, and drilling. We emphasize that such a holistic approach is imperative in order to characterize the tectonic evolution of each region and to link tectonics with seismogenic structures. In the next five sections, we discuss four cases that represent a wide spectrum of tectonics stages, ranging from oblique subduction, to incipient arc–continent collision, and to mature continent–continent collision.

3. Lateral compression in subducted lithosphere

Along subduction zones, the most conspicuous seismogenic structure is the interface between the overriding and subducting plates. Earthquakes that occur along the plate interface typically show thrust faulting with slip being approximately normal to the subduction zone (e.g., Isacks et al., 1968). However, there is now sufficient evidence for an additional seismogenic zone that often occurs within the subducting plate below the plate interface.

Chen and Molnar (1990) first noted that beneath the northern terminus of the Indo-Burma subduction zone, fault plane solutions of large to moderate-sized earthquakes show north–south (N–S) trending compression, sub-parallel to the local strike of the subduction zone where the plate interface itself seems to be aseismic (Ni et al., 1989). Chen and Molnar (1990) interpreted such lateral compression within the subducting lithosphere as a consequence of oblique subduction along the Indo-Burma ranges, so there is a net component of convergence between the northern flank of the subducting Indian lithosphere and the east–west (E–W) trending collision front along the Himalayas.

The distinction between the plate interface and the second seismogenic zone becomes clear in other regions where the plate interface is seismogenic. Through precise determinations of focal depths and fault plane solutions of over 50 earthquakes, Kao and Chen (1991) reported that in southern Ryukyu, a second layer of seismicity shows lateral compression and occurs approximately 10–20 km below the plate interface. Because of oblique subduction toward the northwest, lateral (E–W) compression within the subducting Philippine Sea plate is expected as the E–W trending Ryukyu arc terminates against the N–S trending Taiwan collision zone.

Recently, Kao and Rau (1999) combined travel-time tomography, *S* to *P* conversions, and local seismicity to show that the second layer of seismicity in southern Ryukyu–northern Taiwan indeed occurred below the plate interface and within the down-going slab where *P*-wave speeds are high. More important, they carried out a global survey and documented three analogous cases elsewhere.

One notable case that has not received due attention is the eastern Hellenic trench near the Island of Crete where oceanic lithosphere of the eastern Mediterranean subducts obliquely toward the northeast. Based on geodetic results using the Global Positioning System (GPS) (McClusky et al., 2000), the current convergence between the subducting plate and southwestern Anatolia is about 16 mm/year along an azimuth of N30°E.

Taymaz et al. (1990) studied large to moderate-sized earthquakes along the eastern Hellenic arc in some detail. They noticed that fault plane solutions for half of the 15 events they studied show approximately E–W compression, sub-parallel to the trend of the eastern Hellenic trench. In our view, these events resemble the second layer of seismicity in other zones of oblique subduction. Fig. 1 shows a cross-section based on hypocenters and fault plane solutions reported by Taymaz et al. (1990). The average trend of the *P*-axes is about N100°, nearly perpendicular to the cross-section (along N20°). A major uncertainty here is the position of the plate interface. In the region between the Hellenic trench and Crete, several earthquakes associated with thrust faulting delineate the plate interface, as focal depths and orientation of the shallow-dipping nodal planes mark the position and local dip of the interface, respectively. With one exception (event No. 4), the other six earthquakes all seem to have occurred within the subducted slab (Fig. 1b).

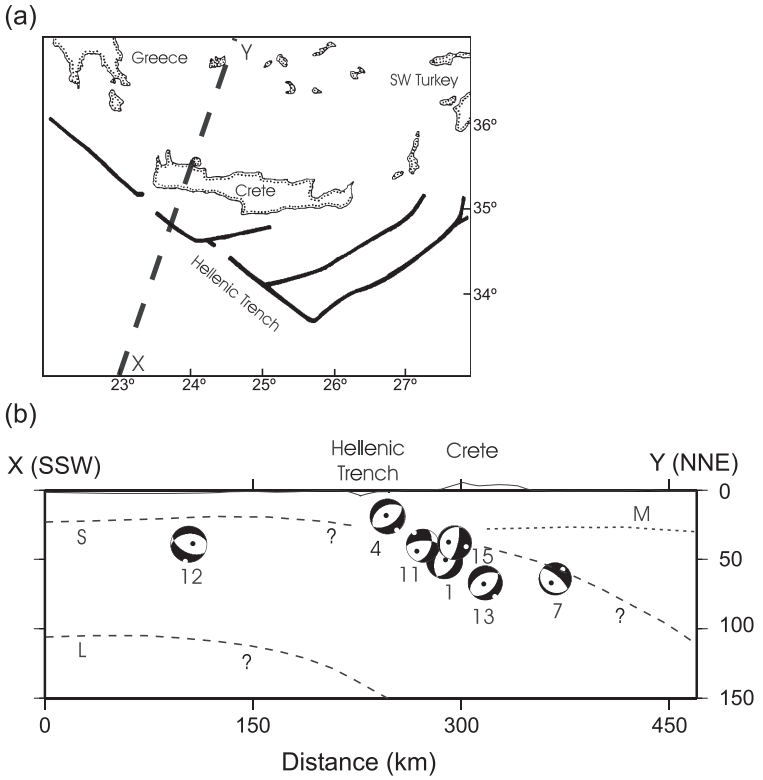

Fig. 1. (a) Simplified map near Crete, showing the location of cross-section (X–Y). Solid curves mark the deepest portion of the Hellenic trench. (b) Cross-section showing fault plane solutions (large symbols) of earthquakes that do not fall along the plate interface. Fault plane solutions are equal-area projections of the back-(western) hemisphere of the focal sphere, with the compression-quadrants darkened. Solid and open circles mark the P- and T-axis of each solution, respectively. Notice that P-axes of these earthquakes are approximately normal to the cross-section, showing lateral compression along the strike of the subduction zone. Labels, "S" and "L" mark the approximate position of the top and bottom of the subducting oceanic lithosphere, respectively, while "M" is the Moho under Crete. Data and base map are from Taymaz et al. (1990).

Thus, the eastern Hellenic subdcution zone seems to be another example where a second seismogenic zone occurs beneath the plate interface, reflecting lateral compression along the flank of a subdcuted slab during oblique convergence. In all, there are now six cases of dual seismogenic zones along the plate interface: eastern Hellenic trench, southern Ryukyu trench, Indo-Burma ranges, New Zealand, southern Cascadia, and eastern Alaska (Kao and Rau, 1999; Kao and Chen, 1991; Chen and Molnar, 1990). Thus, during oblique subduction, a nearby collision zone apparently affects seismogenic structures associated with subduction that are still several hundreds of kilometers away from the collision front. Whereas obliquity of subdcution, not maturity of the nearby collision zone, seems to control lateral compression within subducted slab, earthquakes associated with lateral compression do seem to occur only in the youngest portions of the orogen where *bona fide* subduction is on-going.

4. Equivalence between lateral variation and temporal evolution

The western Taiwan orogen offers a unique opportunity to investigate the transition from *bona fide* subduction to arc–continent collision. Unlike most accretionary wedges, the orogen is largely exposed above sea level, making it accessible to a wide range of field measurements. The Taiwan orogen is a consequence of on-going collision that

began only about 5 Ma ago between the Luzon arc in the western Philippine Sea plate and the passive margin of southeastern China (Fig. 2) (e.g., Suppe, 1988).

Seno et al. (1993) estimated that plate convergence is along N60°W, at a rate of about 70–80 mm/year. Recent geodetic surveys based on GPS indicate approximately the same rate and direction of convergence between Penghu (Pescadores) and the Luzon arc (Yu et al., 1997, Hu et al., 2001). Such a rate is remarkable, since the corresponding rate is only 20–30 mm/year. across the Himalayan collisional front (Bilham et al., 1997)—the world's highest mountain range. The extraordinary rate of convergence across the Taiwan orogen is reflected by abundant seismicity that, in turn, illuminates some intriguing seismogenic structures (Fig. 3).

Due to the oblique nature of the collision in Taiwan, there is a natural progression from subduction in the southwest to full-fledged collision to the northeast. This southward younging of the orogen is evident from the fact that much of the Luzon volcanic arc is yet to collide with Eurasia (e.g., Lutao and Lanhsu; Fig. 2). Suppe (1984) first studied the equivalence between spatial variations of geologic structures and time-progression of the collision process in Taiwan (diachronism). By combining direction of convergence between the Philippine Sea plate and Eurasia, average trend of the passive continental margin, and strike of the suture zone that is approximately parallel to the mountain front, he constructed a triangle, whose sides are to represent velocity vectors of relative motion among stable Eurasia, the collision front, and the Philippine Sea plate. Using estimated rate of convergence between the Philippine Sea plate and Eurasia (thus fixing the magnitude of each vector), Suppe (1984) inferred that the collision front moves at a rate of about 84 mm/year toward the southern end of the fold-and-thrust belt (cf. Fig. 4).

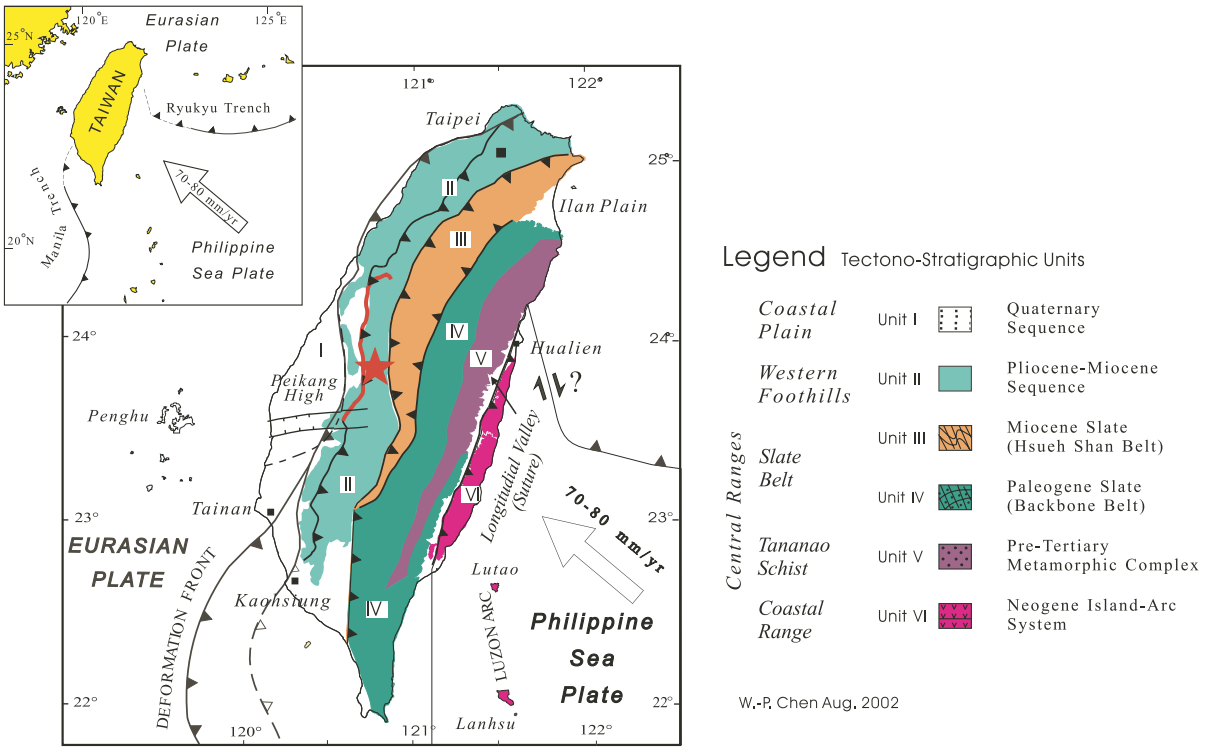

Fig. 2. Map showing major tectono-stratigraphic units and the overall setting (inset) of the Taiwan orogen. The large asterisk marks the epicenter of the Chi-Chi sequence while the thick curve is the surface break associated with this sequence. Courtesy of Jian-Cheng Lee, Institute of Earth Sciences, Academia Sinica, Taiwan.

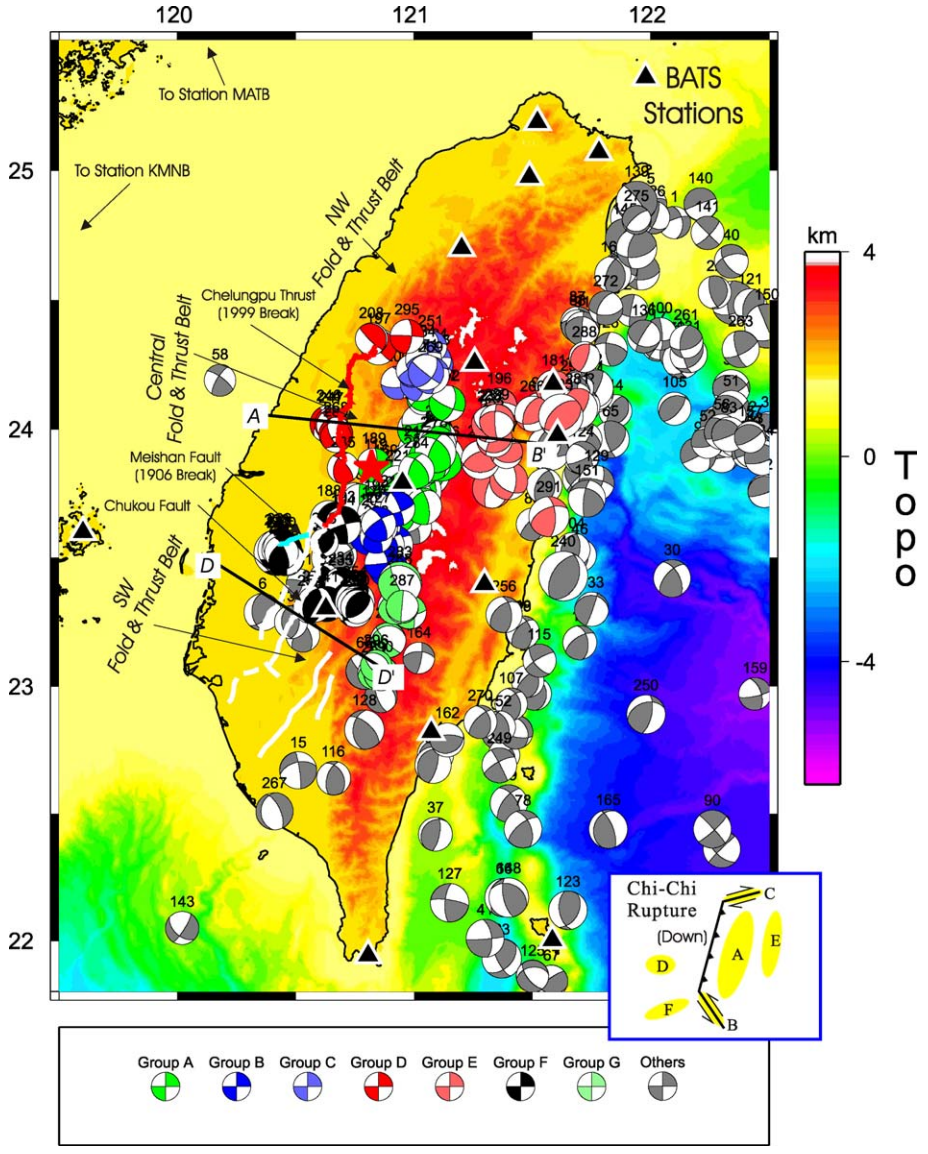

Fig. 3. Map showing topography/bathymetry and recent seismicity near Taiwan. Solid triangles mark broadband seismic stations of Broadband Array in Taiwan for Seismology (BATS). Two additional stations are located on isles (under Taiwanese jurisdiction) near the coast of southeastern China. Large symbols are preliminary BATS fault plane solutions numbered in chronological order (in equal-area projection of the lower hemisphere of the focal sphere, with the compression-quadrants darkened). Shading of fills in fault plane solutions reflects grouping of events. Only events in Groups A, B, and C are directly related to the Chi-Chi sequence (Kao and Chen, 2000). The lower inset shows the hanging wall of the Chelungpu thrust moved westward, terminating laterally at strike-slip zones marked by aftershocks in Groups B and C. Also shown are surface break associated with the sequence in central Taiwan (thick curve), and known active faults in southwestern Taiwan (white curves). Notice the obvious change in structural trends near 23.7°N. AB′ And DD′ mark locations of cross-sections shown in Figs. 6 and 5, respectively.

Recent geodetic results based on GPS, however, showed that there is considerable contraction, over 55 mm/year, between the Luzon arc and the suture zone (Yu et al., 1997, Hu et al., 2001). So we revise the space–time equivalence along the western Taiwan orogen by using the observed, uniform velocity

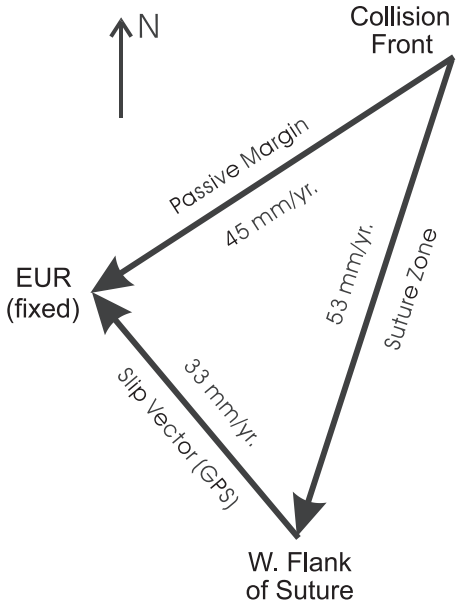

Fig. 4. Velocity vectors relevant to the equivalence between time and space along the western Taiwan orogen. Based on GPS data, the western flank of the suture zone has a uniform velocity of current convergence toward stable Eurasia (“EUR”). The collision front migrates toward the southwest at 40–50 km/Ma. This estimate supersedes that of Suppe (1984) who did not have information about extensive internal deformation between the Luzon arc and the suture zone.

of current convergence between the western flank of the suture zone and Eurasia (~ 33 mm/year, Fig. 4). The resulting rate for the migration of the collision front is about 53 mm/year toward the south–southwest. In other words, a change in distance of 50 km along the western Taiwan orogen is equivalent to about 1 Ma in temporal evolution of the collision process.

5. Incipient arc–continent collision and reactivation of normal faults

South of about 21.5°N, an active subduction zone accompanies the Manila trench. Between 21.5 and 23°N, there is a gradual transition from subduction to collision, a process accomplished by distributed thrust faulting in the frontal portion of the accretionary prism, closing of the fore-arc basin, and internal deformation of the Philippine Sea plate (Kao et al., 2000). Near 23°N, the deformation front extends northward on-shore and continues as the fold-and-thrust belt in southwestern Taiwan (Fig. 2).

In several ways, this belt in southwestern Taiwan is distinct from its northward counterpart in central Taiwan. South of about 23.7°N, the fold-and-thrust belt broadens while the slate belt of Miocene deposits pinches out (Fig. 2). The trend of the fold-and-thrust belt also turns by about 30°, from nearly N–S to north–northeast/south–southwest (Fig. 2). Surface break of the Chi-Chi earthquake also terminates abruptly near 23.6°N (Fig. 3).

Suppe (1981) proposed a sequence of shallow-rooted ramp thrusts and fault-bend folds in southwestern Taiwan to explain structural data mapped mainly near the surface. This forms the basis of the well-known critical taper model where a basal detachment fault of low frictional strength (“basal decollement”), dipping at a small angle of 5–6°, was proposed as the controlling geologic structure (Davis et al., 1983). The critical taper model is a mainstay of thin-skinned tectonics, contending that deformation occurs only in a wedge of deformed sediments and sedimentary rocks above the basal decollement. The wedge is at a critical state in that its state of stress, controlled mainly by its shape and the frictional strength of the basal decollement, is everywhere near the Mohr-Coulomb criterion of failure.

In such a view, there is no fundamental change in the style of deformation between fold-and-thrust belts in central and southwestern Taiwan (Davis et al., 1983). So the critical taper model cannot account for obvious changes in regional structural trends and styles (Fig. 2). There are a number of indications that reactivation of structures, that were originally associated with extension of the passive continental margin, is important—an alternative supported by focal depths and fault plane solutions of recent seismicity (Fig. 5).

Extensive work related to the exploration of hydrocarbons showed that geologic structures related to the opening of the South China Sea are preserved beneath the southwestern coastal plains. Extensional structures, including several normal fault systems, extend offshore and form part of a large-scale basin, characteristic of rifted margins (Lee and Lawver, 1994; Yang et al., 1991; Yeh and Yang, 1994). Considering that the rifted margin abuts the foothills

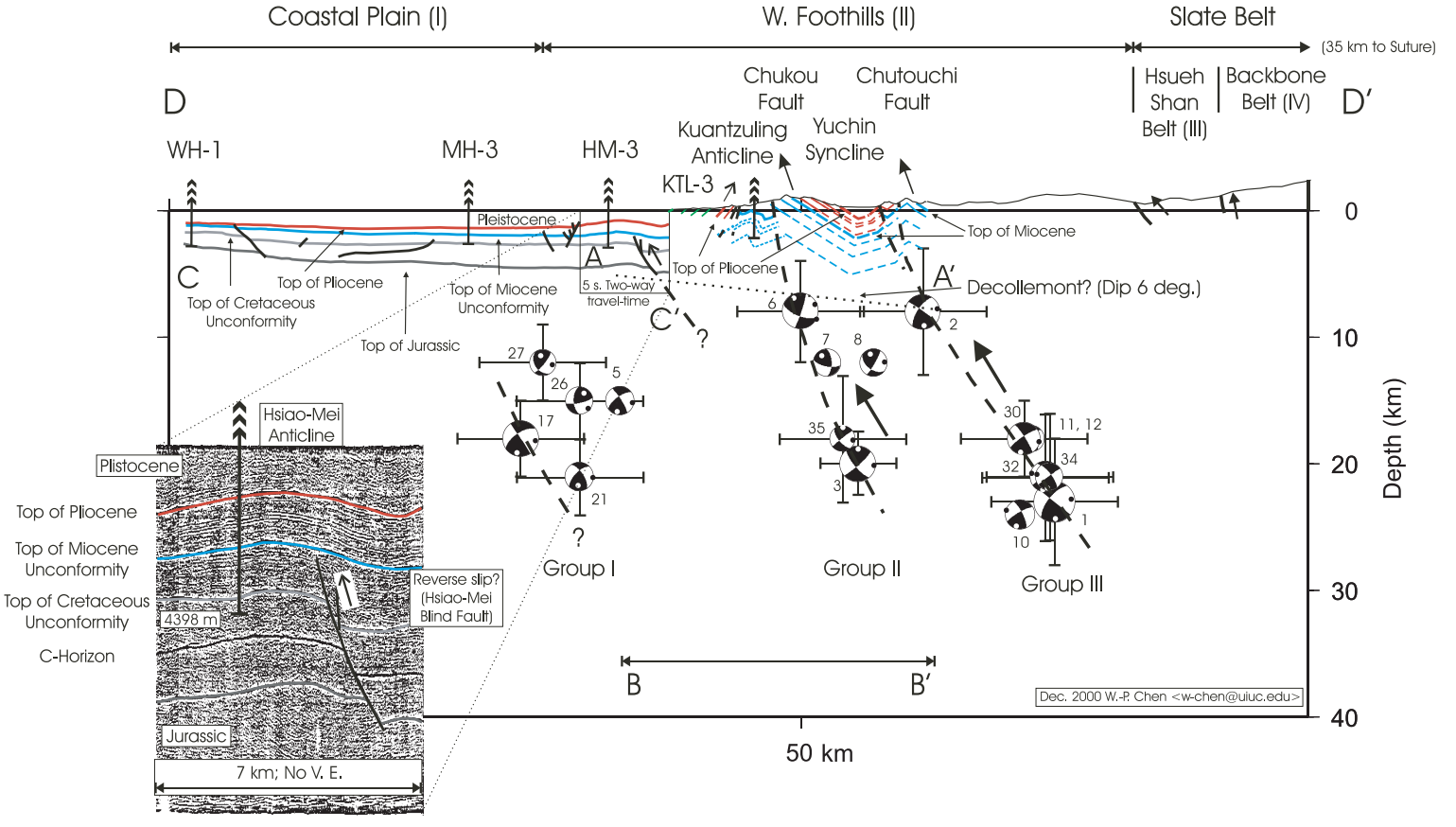

Fig. 5. Cross-section of the fold-and-thrust belt in southwestern Taiwan (DD′ , Fig. 3), showing our interpretation of the relationship between subsurface geology and seismogenic faulting at depth. The inset shows a seismic profile over the Hsiao-Mei anticline (Chow et al., 1992) where reverse slip appears to occur along a pre-existing normal fault. Focal depths and moderate- to steep-dipping nodal planes (45–60°) suggest that deformation occurs below the decollement, along high-angle faults that connects to known faults near the surface. Layout of fault plane solution is the same as that in Fig. 1.

of southwestern Taiwan (Fig. 2), it is natural to suspect that normal faults are being reactivated in the youngest portion of the collision zone.

Based on drilling and retro-deformable cross-sections in key regions where multiple ramp-thrust systems were originally proposed, Chang et al. (1996) contended that reverse slip on high-angle faults is the main cause of the fold-and-thrust belt in southwestern Taiwan. It is interesting to note that Chang was involved in postulating the thin-skinned model for western Taiwan (Suppe and Chang, 1983). Indeed it has been known for some time that reliably determined focal depths indicate active deformation deep in the crust to depths of about 25 km (Huang et al., 1996; Wu et al., 1997). This is direct evidence to refute a key assumption of the critical taper model where no deformation should occur below the basal decollement.

Since the devastating Chi-Chi earthquake sequence of 1999, seismicity increased remarkably in southwestern Taiwan. Fig. 5 summarizes a comprehensive compilation of precisely determined earthquake parameters (Chen and Kao, 2000b). Most fault plane solutions show reverse faulting on moderate- to steep-dipping planes (>45°), considerably steeper than either thrust faulting during the largest shocks of the Chi-Chi sequence (20–30°, Fig. 6) farther to the north or the basal detachment (6°) (Fig. 5). The consistency among fault plane solutions indicates that high-angle reverse faulting is a dominant mode of deformation. Trends in hypocenters are generally consistent with orientations of nodal planes such that seismogenic reverse faulting at mid-crustal depths seems to be connected with surface traces of well-known faults (Fig. 5).

Important clues to the nature of faulting are also contained in published results of drilling and seismic reflection profiles. For instance, the Hsiao-Mei anticline lies immediately to the west of the Chukou fault, a well-known active fault (Figs. 3 and 5). Beneath this anticline, a high-angle blind fault apparently originated as a normal fault in the Paleogene, as it offset strata of Cretaceous and Jurassic age but did not penetrate the top of the Miocene unconformity (inset of Fig. 5). Compressional overprinting of this particular fault is strongly suggested by the observation that strata as old as the Jurassic and as young as the Pliocene to recent are involved in folding (inset of Fig. 5). This type of structure is indicative of reverse slips along pre-existing normal faults and we interpret that the imbricate, high-angle, seismogenic faults beneath southwestern Taiwan originated as normal faults along the passive margin of southeastern China. Apparently, inversion of sedimentary basins is ongoing at mid- to lower crustal depths.

It is interesting to note that for a given amount of horizontal contraction, high-angle reverse faults produce much more uplift than low-angle thrusts. This may explain why incipient collision already caused a higher average elevation (~ 1 km) in southwestern Taiwan than in central Taiwan (~ 0.75 km) where the collision is more mature.

6. Out-of-sequence thrusts

The main shock of the Chi-Chi earthquake sequence occurred on September 20, 1999 beneath the central portion of the western Taiwan orogen. A clear surface rupture extends from 23.6 to 24.3°N (Figs. 2 and 3). Near the surface, several meters of slip occurred along the Chelungpu thrust that dips to the east at 20–30° . Even though this thrust was believed to have originated as a listric fault (Davis et al., 1983), a planar extension of this thrust from the surface to a depth of about 15 km provides a straightforward explanation for the main rupture of the Chi-Chi sequence.

First, an average dip of 25° of the Chelungpu thrust is consistent with the range of apparent dips of the fault plane (20–30°) of the largest events (S2–S4 and T4) (Fig. 6). Second, the centroids of these events cluster around such a planar structure. Notice that while focal depths of the main shock have large uncertainties because of the complex rupture history, the depth of the largest aftershock, T4, is well constrained. Thus, a major planar thrust seems to cut cross the detachment and extends down to mid-crustal depths (Fig. 6). Note that the deformation front now is clearly to the west of the Pakuashan ramp thrust (Fig. 6). Thus, the seismogenic structure is an out-of-sequence thrust system that develops or remains active in the hinterland of the deformation front (e.g., Morely, 1988; Boyer, 1992).

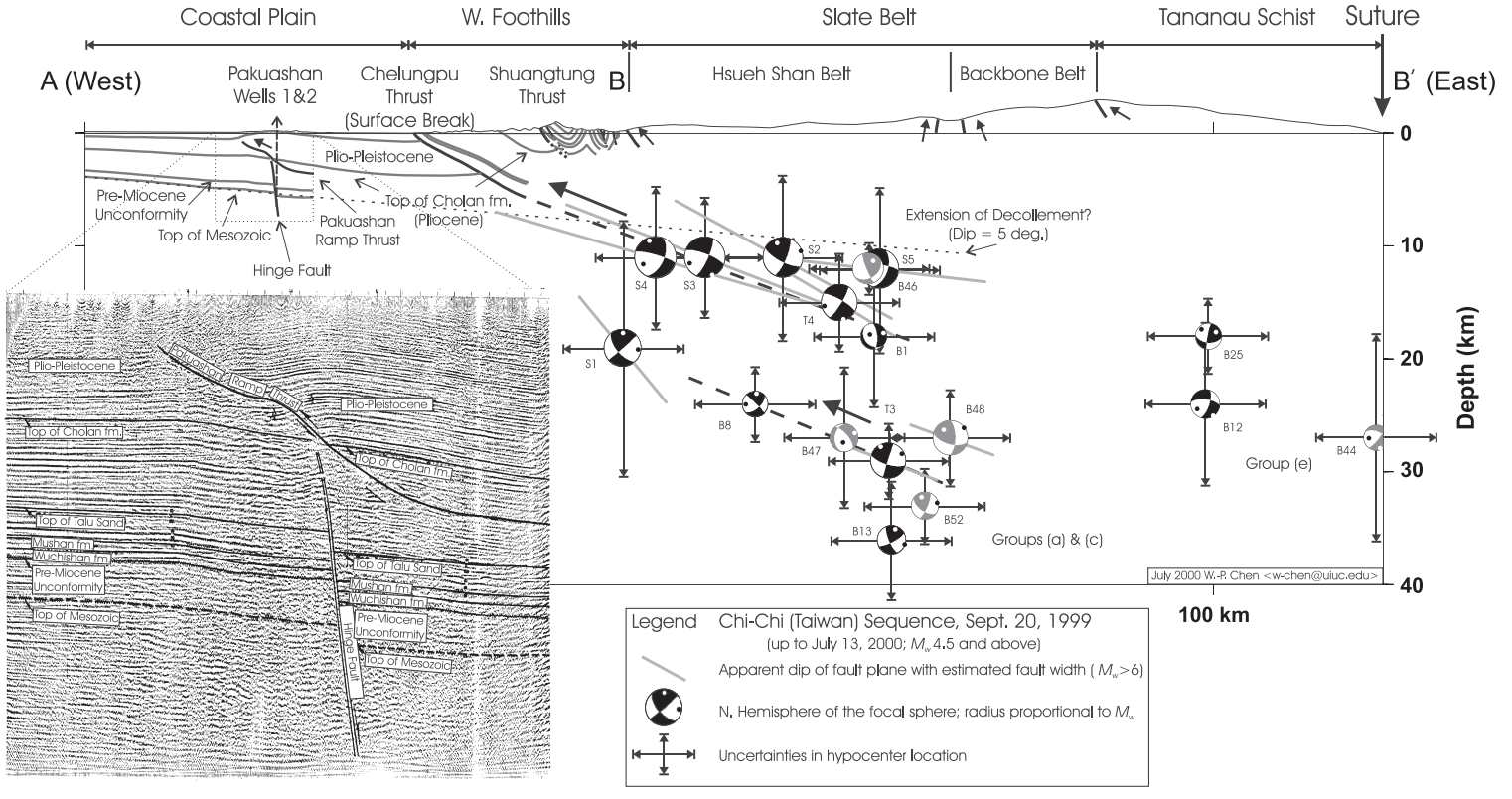

Fig. 6. Cross-section of the central Taiwan orogen (AB′, Fig. 3), showing the relationship between subsurface geology beneath the foreland (Chiu, 1971; Hsiao, 1968), and seismogenic zones of the Chi-Chi sequence at depth. For the largest events, gray lines show estimated width of each rupture based on its seismic moment and a static stress drop of 10 MPa (see text for formula). The inset shows a seismic profile of particular interest (Chen, 1978). For clarity, we include only large events of M_w over 4.5. The active Chelungpu thrust that broke the surface during the sequence is an out-of-sequence fault, evident from the deformation farther west, including the Pakuashan ramp thrust and the overlying fault-bend anticline. A planar extension of the Chelungpu thrust explains apparent dips of fault planes and depths for the largest shocks in the Chi-Chi sequence. Another deeper seismic zone is also apparent down to depths over 30 km. Both relic normal faults (e.g., hinge fault in insert) and the basal decollement appear to be aseismic. Layout of fault plane solution is the same as that in Fig. 1. Adapted from Chen and Kao (2000a).

A remarkable feature of the Chi-Chi sequence is the long-lasting, strong aftershocks (M_w>6). The sequence remains quite active after 9 months, evident from a large (M_w 6.1), late aftershock on June 10, 2000 (Chen and Kao, 2000a). The large aftershocks indicate a second seismogenic zone beneath the main, out-of-sequence thurst. The strongest evidence is the difference in depths of about 15 km between two large aftershocks, T3 and T4 (Fig. 6). The two epicenters are next to each other, yet the two events show a difference of over 8 s in the time interval *sS*–*S*, the differential arrival time between the direct *S*-wave arrival and the reflection off the free-surface above the hypocenter, *sS* (Kao and Chen, 2000; their Fig. 2). On June 10, 2000, an event of M_w 6.1 (B48), the largest since September 25, 1999, occurred in the same general area. Both focal depths and fault plane solutions for events T3 and B48 are similar (Fig. 6), lending further credence to a second, deep-seated seismogenic zone.

The depths of large events T3 and B48 alone suggest that these events do not belong to the same cluster as events S2–S5 and T4 (Fig. 3). Furthermore, apparent dips of the east-dipping nodal plane for events T3, B48 and B8 are also close to 25°, suggesting that a planar structure extends up-dip from event T3 by a depth of about 15 km, forming a second, deeper seismic zone (Kao and Chen, 2000). Remarkably, results for events B47 (May 18, 2000), B48 (June 10, 2000), and B52 (June 19, 2000) fall close to this structure as predicted from data prior to February 7, 2000. With the additional information from late, large aftershocks in May and June of 2000, there seems little doubt that the Chi-Chi sequence is associated with a system of multiple reverse faults (Fig. 6) (Chen and Kao, 2000a).

It is important to point out that both focal depths and fault plane solutions shown in Figs. 5 and 6 are highly precise, because results from the inversion of regional waveforms have been calibrated by well-established technique from the inversion of teleseismic data (Kao and Chen, 2000). Furthermore, we plotted estimated widths of earthquake rupture in Fig. 6 so one has an intuitive understanding of how much of the fault actually slipped in each event or sub-event. Assuming a circular rupture, radius of rupture (r) equals $(7M_o/16\Delta\sigma)^{1/3}$, where M_o and $\Delta\sigma$ are the seismic moment and the static stress drop, respectively. Notice that even if $\Delta\sigma$ is off by a factor of 10, r changes only by a factor of two. So our main basis for identifying the dual, seismogenic thrusts is the combination of apparent dips of nodal planes and estimated rupture widths. Contrary to the common practice connecting hypocenters, our approach has a clear physical basis (Brudzinski and Chen, 2003).

While seismogenic thrust faulting has been observed down to 30–40 km in other zones of continental convergence (Chen and Molnar, 1983), those cases involve moderate-sized events that cannot be easily associated with known geologic features. In contrast, results from the Chi-Chi sequence suggest that seismogenic faulting occurs along well-defined structures near the surface and reaches down to depths of about 30 km. A set of out-of-sequence thrusts that reach down to mid- or lower crustal depths has never been well documented elsewhere and illustrates how some important seismogenic structures cannot be reliably extrapolated from observations near the surface.

Recently, Wu et al. (2003) relocated aftershocks of the Chi-Chi sequence and reported a cluster of small earthquakes near event B48 that form a steep-dipping band toward the west. If this band of small aftershocks occur along the true fault plane, then one must allow for the possibility that the second layer of seismicity shown if Fig. 6 may have occurred on a system of deep-seated reverse faults conjugate to the rupture of the main shock.

In any case, the pattern of faulting associated with the Chi-Chi sequence is distinct from that in southwestern Taiwan (cf. Figs. 5 and 6). Based on the distribution and the fault plane solution of aftershocks, Kao and Chen (2000) reported that the main rupture of the Chi-Chi earthquake terminated at zones of strike-slip faulting which accommodate westward slip of the hanging wall. The southern zone of accommodation shows left-lateral slip, trending north–northwest/south–southeast (Fig. 3, inset). This trend intersects the axis of the southwestern fold-and-thrust belt at a high angle (~ 60°). Thus, the segmented nature of the fold-and-thrust belt in western Taiwan seems clear (Figs. 2 and 3) (Rubin et al., 2001). Although one can never rule out other contributing factors, the simplest explanation is that such lateral variations mainly reflect time-progression of the orogen. Since the length of the fold-and-thrust belt in

southwestern Taiwan is less than 100 km, the transition from reactivation of high-angle faults to dual thrusts requires only 2–3 Ma in the history of this collision zone (Fig. 4).

7. Mantle earthquakes during continent–continent collision

Twenty years ago, Molnar and Chen (1982) suggested a case of dual, seismogenic thrusts for the Himalayan collision zone but could not rule out alternative interpretations (Baranowski et al., 1984). Nonetheless, recent seismicity along the Himalayas clearly demonstrates the importance of deep-seated seismogenic structures that have no clear expressions near the surface.

A case in point is the large ($M_w \sim 6.7$) earthquake of August 20, 1988 near the Nepali–Indian border, killing over 2000 people and causing widespread damage as far south as New Delhi. Using broadband data recorded at teleseismc distances, Chen and Kao (1996) studied this event in detail and showed that it occurred beneath the foreland of the Himalayas at a depth of 51 ± 5 km, likely in the uppermost mantle of the Indian shield (Fig. 7).

The Himalayan–Tibetan orogen is a mature intracontinent convergent zone, formed by the collision between Eurasia and India since about 50 Ma ago (e.g., Molnar and Tapponnier, 1975; Yin and Harrison, 2000). In general, known geologic structures along the Himalayas are similar to other large-scale contraction belts, with a fold-and-thrust belt that involves progressively greater degree of deformation and metamorphism from the foreland to the hinterland (Fig. 7). A longstanding view is wholesale underthrusting of the Indian shield beneath the Himalayas and southern Tibet (Argand, 1924). This view received renewed interest when seismic reflection profiles show two sets of deep-seated reflectors under the Tethyan Himalayas (Fig. 7). Although there is no evidence to show that these reflectors are active faults or shear zones, it is geometrically plausible to connect the top reflector and estimated position of the top of the Indian shield in the foreland, forming a hypothetical mega-thrust that underlies the entire Himalayas (Zhao et al., 1993, Hauck et al., 1998). Such a mega-thrust is equivalent to the plate interface along subduction zones or the basal decollement in the critical taper model. In this scenario, the mega-thrust would be the sole, dominant seismogenic structure with no deformation below it.

In contrast, there are several competing hypotheses that involve deformation of the entire crust and perhaps even the uppermost mantle. For instance, early seismic work suggested that there are offsets in the Moho beneath the Tethyan Himalayas and southern Tibet (Hirn et al., 1984). This preliminary result and analog modeling lead Burg et al. (1994) to propose that deformation in the upper crust and in the uppermost mantle are brittle but decoupled from each other by a weak, ductile lower crust. If the steep-dipping nodal plane of the large earthquake on August 20, 1988 is the true fault plane (Fig. 7), it serves as the modern analogue of how offsets in the Moho may have developed and been transported farther to the north.

It is interesting to note that the rheology of a weak, ductile lower crust being sandwiched between brittle upper crust and uppermost mantle has a broad observational basis: there are several intra-continental regions with two distinct layers of seismicity, one in the upper crust and one in the uppermost mantle (Chen and Molnar, 1983). A clear example is southern Tibet, where a number of mantle earthquakes have occurred at depths of about 90 km (Fig. 7). However, fault plane solutions of mantle earthquakes are nearly identical to those of shallow seismicity in the upper crust (5–10 km), all showing east–west extension (Molnar and Chen, 1983, Chen and Kao, 1996). Thus, the upper crust and the uppermost mantle seem to be coupled somehow. Currently, there is a renewed debate on whether a strong uppermost mantle underlies the continental lithosphere (e.g., Jackson, 2002). While a comprehensive discussion of this issue is beyond the scope of this paper, it is important to note that deep seismicity in southern Tibet is most likely in the uppermost mantle, as precisely determined crustal thickness is merely 66 ± 3 km over these moderate-sized earthquakes (Fig. 7) (Mejia, 2001).

Lyon-Caen and Molnar (1983, 1985) used gravity profiles to study the flexure of lithosphere and proposed that the Himalayas comprised of a sequence of crustal nappes. The first nappe developed and moved along the Main Central Thrust (MCT), a major ramp thrust that broke the entire crust. Subsequently, a

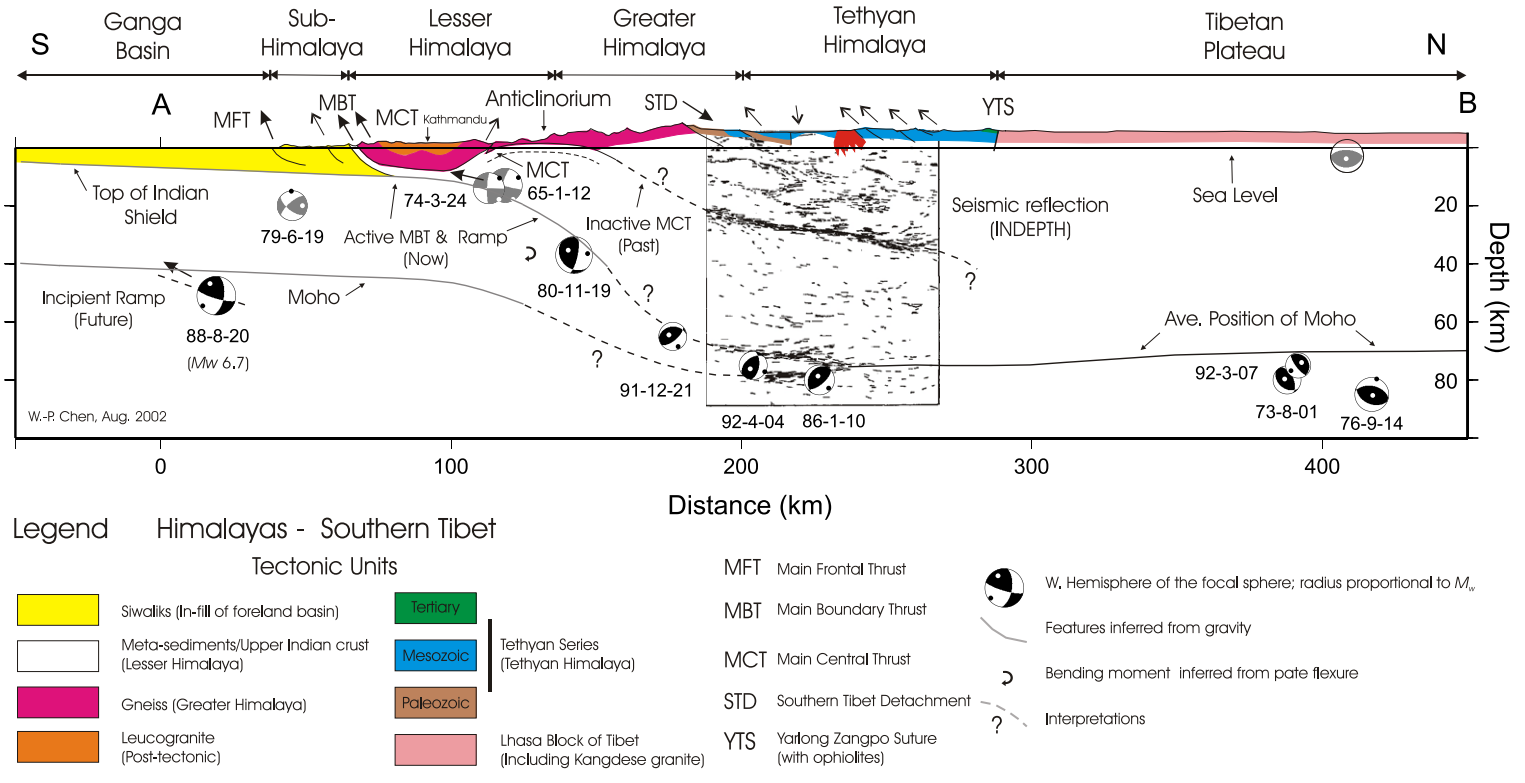

Fig. 7. A north–south cross-section of the Himalayan–Tibetan orogen, summarizing current information regarding the top 100 km of lithospheric deformation. Notice sub-crustal earthquakes are common beneath both the foreland and the hinterland, highlighting the importance of linking concurrently active deformation through the entire thickness of the lithosphere. At the moment, key information is missing beneath the Greater Himalaya, allowing several alternative interpretations. Layout of fault plane solution is the same as that in Fig. 1. Sources of data are earthquakes (Chen and Kao, 1996), modeling of plate flexure and gravity (Lyon-Caen and Molnar, 1983, 1985; Jin et al., 1996), seismic reflection (Hauck et al., 1998), crustal thickness from joint inversion of receiver functions and surface wave dispersion (Mejia, 2001), and geologic mapping (Gansser, 1977; Burchfiel et al., 1992; Pandey et al., 1995).

second nappe formed along the Main Boundary Thrust as the mountain front propagated toward the foreland. In this view, the large earthquake beneath the Moho in the foreland may mark the initiation of a third nappe (Fig. 7), if the shallow-dipping nodal plane is the true fault plane.

At the moment, support for a shallow dipping fault plane associated with this sub-crustal earthquake beneath the foreland comes only from the distribution of aftershocks and background seismicity that forms a broad pattern in map-view (National Seismological Center, 1997), inconsistent with a high-angle seismogenic fault. Moreover, recent isotopic studies questioned the role of the MCT as a crustal nappe, because isotopic signature of the hanging wall, the Greater Himalayas, does not seem to resemble that of the Indian shield (see, for instance, a recent, comprehensive review by Yin and Harrison (2000) and extensive references therein). Thus, it seems premature to set on a unique interpretation.

Another key issue is the complete lack of subsurface data beneath the Greater Himalayas, so the critical link between the intact Indian shield and the mobile Tibetan lithosphere is missing. Nevertheless, available earthquake data clearly demonstrate the important role of active deformation in the uppermost mantle throughout the mature Himalayan–Tibetan collision zone (Fig. 7). Thus, the controversy of thin-skinned (e.g., critical taper) versus lithoshperic deformation (e.g., crustal nappes) seems too restrictive and even misguided. We advocate the perspective of understanding the link between deformation near the surface and that at depth, as both clearly are concurrently active throughout the evolution of collision zones (Figs. 5–7).

8. Discussions and conclusions

We discuss seismogenic structures of four regions whose tectonic stages range from oblique subduction prior to collision, to incipient arc–continent collision, to mature continent–continent collision. In each case, deep-seated seismogenic faulting occurs on features that are unexpected from known geologic information gathered near the surface. Indeed, it requires little extrapolation to illuminate seismogenic structures with high-resolution earthquake data, as these structures are currently producing earthquakes and fault plane solutions provide excellent kinematic indicators at depth. On the other hand, modern seismic data have a limited span of at most four decades in time, an interval far shorter than the average recurrent interval of major earthquakes (e.g., Yeats et al., 1997).

In this study, we take the perspective that a collision zone's maturity along its temporal path of tectonic evolution is an important factor in controlling seismogenic structures. For earthquakes reflecting lateral compression near the termini of zones of oblique subduction, the main strength of our reasoning lies in the number of such cases globally (Fig. 1) (Taymaz et al., 1990; Chen and Molnar, 1990; Kao and Chen, 1991; Kao and Rau, 1999).

For young, oblique collision between an island arc and a passive continental margin, the equivalence between spatial variations and temporal evolution along the western Taiwan orogen illustrates how in just a few million years, seismogenic structures shift from concentrated slip along the plate interface (basal decollement) of subduction zones (Kao et al., 2000), to distributed, reverse slip along high-angle normal faults (Fig. 5), to motion along out-of-sequence thrusts that reach mid- to lower crustal levels (Fig. 6).

For the mature Himalayan–Tibetan collision zone, major, crustal scale geologic structures in general and seismogenic faulting in particular are controversial because critical data are missing beneath the Greater Himalayas. Nonetheless, damaging earthquakes in the uppermost mantle point to need for understanding how concurrent deformation in the upper crust and the uppermost mantle is coupled (Fig. 7).

Acknowledgements

T. Taymaz and S. Ozalaybey, co-conveners of the workshop in May of 2002 on active faulting and continental deformation in seismogenic zones of the eastern Mediterranean region, encouraged us to write up this article. The two conveners, R. Westaway, and H. Kao also provided many helpful discussions. We thank G. Houseman, J. Kasahara and W. P. Leeman for reviewing the manuscript. This material is based on work supported by the National Science Foundation under Grants No. EAR0106786 and EAR9909362 (Project Hi-CLIMB: An Integrated Study of the *Hi*malayan–T*i*betan *C*ontinental *Li*thosphere during

*M*ountain *B*uilding). Any opinions, findings and conclusions or recommendations expressed in this material are those of the authors and do not necessarily reflect those of the National Science Foundation.

References

Argand, E., 1924. La tectonique de l'Asie. Int. Geol. Cong. Rep. Sess. 13, 170–372.

Baranowski, J., Armbruster, J., Seeber, L., Molnar, P., 1984. Focal depths and fault plane solutions of earthquakes and active tectonics of the Himalaya. J. Geophys. Res. 89, 6918–6928.

Bilham, R., Larson, K., Freymueller, J., 1997. GPS measurements of present-day convergence across the Nepal Himalaya. Nature 386, 61–64.

Brudzinski, M.R., Chen, W.-P., 2003. Visualization of seismicity along subduction zones: toward a physical basis. Seismol. Res. Lett. 74, 731–738.

Boyer, S., 1992. Sequential development of the southern Blue Ridge province of northwest North Carolina ascertained from the relationships between penetrative deformation and thrusting. In: Mitra, S., Fisher, G. (Eds.), Structural Geology of Fold and Thrust Belts. Johns Hopkins Univ. Press, Baltimore, MD, pp. 161–188.

Burchfiel, B.C., Chen, Z.-L., Hodges, K.V., Liu, Y.-P., et al., 1992. The South Tibet Detachment System, Himalayan orogen: extension contemporaneous with and parallel to shortening in a collisional mountain belt. Spec. Pap. Geol. Soc. Am. 269, 1–41.

Burg, J.-P., Davy, P., Martinod, J., 1994. Shortening of analogue models of the continental lithosphere: new hypothesis for the formation of the Tibetan plateau. Tectonics 13, 475–483.

Chang, Y.-L., Lee, C.-I, Lin, C.-W., Hsu, C.-H., Mao, E.-W., 1996. Inversion tectonics in the fold-and-thrust belt of the foothills of the Chiayi-Tainan area, southwestern Taiwan. Pet. Geol. Taiwan 30, 163–176.

Chen, J.-S., 1978. A comparative study of the refraction and reflection seismic data obtained on the Changhua plain to the Peikang shelf. Pet. Geol. Taiwan 15, 199–217.

Chen, W.-P., Kao, H., 1996. Seismotectonics of Asia: Some recent progress. In: Yin, A., Harrison, M. (Eds.), The Tectonic Evolution of Asia. Cambridge Univ. Press, Palo Alto, pp. 37–62.

Chen, W.-P., Kao, H., 2000a. Evidence for dual, out-of-sequence thrust faulting during the Chi-Chi (Taiwan) earthquake sequence of 1999. Int. Workshop on Annual Commemoration of the Chi-Chi Earthquake. Nat. Center Res. Earthquake Engineer, Taipei, pp. 71–81.

Chen, W.-P., Kao, H., 2000b. Seismogenic reverse faulting in southwestern Taiwan: inversion tectonics at mid-crustal depths (Abstract). EOS Trans. Am. Geophys. Union 81, F883.

Chen, W.-P., Molnar, P., 1983. Focal depths of intracontinental and intraplate earthquakes and their implications for the thermal and mechanical properties of the lithosphere. J. Geophys. Res. 88, 4183–4214.

Chen, W.-P., Molnar, P., 1990. Source parameters of earthquakes and intraplate deformation beneath the Shillong plateau and the northern Indoburman ranges. J. Geophys. Res. 95, 12527–12552.

Cheng, S.N., Yeh, Y.T., Hsu, M.T., Shin, T.C., 1999. Photo Album of Ten Disastrous Earthquakes in Taiwan. Central Weather Bureau and Academia Sinica, Taipei.

Chiu, H.T., 1971. Folds in the northern half of western Taiwan. Petrol. Geol. Taiwan 8, 7–19.

Chow, J., Chang, T.-Y., Liang, S.-C., Shen, H.-C., 1992. Geophysical study on Pre-Miocene hydrocarbon traps around the Peikang area. Pet. Geol. Taiwan 27, 153–175.

Davis, D., Suppe, J., Dahlen, F.A., 1983. Mechanics of fold-and-thrust belts and accretionary wedges. J. Geophys. Res. 88, 1153–1172.

Gansser, A., 1977. The great suture zone between Himalaya and Tibet. Himalaya: Science de la Terre. Centre National de la Recherche Scientifique, Paris, pp. 181–192.

Hauck, M.L., Nelson, K.D., Brown, L.D., Zhao, W.-J., Ross, A., 1998. Crustal structure of the Himalayan orogen at ~90 east longitude from Project INDEPTH deep reflection profiles. Tectonics 17, 481–500.

Hirn, A., Nercessian, A., Sapin, M., Jobert, G., et al., 1984. Lhasa block and bordering structures–a continuation of a 500-km Moho traverse through Tibet. Nature 307, 25–27.

Hsiao, P.-T., 1968. Seismic study of the Taichung area, Taiwan. Pet. Geol. Taiwan 6, 209–218.

Hu, J.-C., Yu, S.-B., Angelier, J., Chu, H.-T., 2001. Active deformation of Taiwan from GPS measurements and numerical simulations. J. Geophys. Res. 106, 2265–2280.

Huang, B.-S., Chen, K.-C., Yeh, Y.T., 1996. Source parameters of the December 15, 1993 Tapu earthquake from first-P motions and waveforms. J. Geol. Soc. China 39, 235–250.

Isacks, B., Oliver, J., Sykes, L.R., 1968. Seismology and the new global tectonics. J. Geophys. Res. 73, 5855–5899.

Jackson, J., 2002. Strength of the continental lithosphere: time to abandon the jelly sandwich? GSA Today, 4–10 (Sept.)

Jin, Y., McNutt, M.K., Zhu, Y.-S., 1996. Mapping the descent of Indian and Eurasian plates beneath the Tibetan plateau from gravity anomalies. J. Geophys. Res. 101, 11275–11290.

Kao, H., Chen, W.-P., 1991. Earthquakes along the Ryukyu–Kyushu Arc: Strain segmentation, lateral compression and the thermomechanical state of the plate interface. J. Geophys. Res. 96, 21443–21485.

Kao, H., Chen, W.-P., 2000. The Chi-Chi earthquake sequence: active, out-of-sequence thrust faulting in Taiwan. Science 288, 2346–2349.

Kao, H., Rau, R.-J., 1999. Detailed structures of the subducted Philippine Sea plate beneath northeast Taiwan: a new type of double seismic zone. J. Geophys. Res. 104, 1015–1033.

Kao, H., Huang, G.-C., Liu, C.-S., 2000. Transition from oblique subduction to collision in the northern Luzon arc–Taiwan region: constraints from bathymetry and seismic observations. J. Geophys. Res. 105, 3059–3079.

Lee, T.-Y., Lawver, L., 1994. Cenozoic plate reconstruction of the South China Sea region. Tectonophysics 235, 149–180.

Lyon-Caen, H., Molnar, P., 1983. Constraints on the structure of the Himalaya from an analysis of gravity anomalies and a flexural model of the lithosphere. J. Geophys. Res. 88, 8171–8191.

Lyon-Caen, H., Molnar, P., 1985. Gravity anomalies, flexure of the Indian plate, and the structure, support and evolution of the Himalaya and Ganga basin. Tectonics 4, 513–538.

McClusky, S., Balassanian, S., Barka, A., et al., 2000. Global Positioning System constraints on plate kinematics and dynamics in the eastern Mediterranean and Caucasus. J. Geophys. Res. 105, 5695–5719.

Mejia, J.A., 2001. Lithospheric structure beneath the Tibetan plateau using simultaneous inversion of surface wave dispersion and receiver functions. PhD thesis, St. Louis Univ., 296 pp.

Molnar, P., Chen, W.-P., 1982. Seismicity and mountain building. In: Hsü, K. (Ed.), Mountain Building Processes. Academic Press, San Diego, CA, pp. 41–57.

Molnar, P., Chen, W.-P., 1983. Depths and fault plane solutions of earthquakes under the Tibetan plateau. J. Geophys. Res. 88, 1180–1196.

Molnar, P., Tapponnier, P., 1975. Cenozoic tectonics of Asia: effects of a continental collision. Science 189, 419–426.

Morely, C.K., 1988. Out-of-sequence thrusts. Tectonics 7, 539–561.

Nábelek, J.L., 1984. Determination of earthquake source parameters from inversion of body waves. PhD thesis, Mass. Inst. of Technol., Cambridge, MA.

National Seismological Center, 1997. Microseismic epicenter map of Nepal HImalaya and adjoining region. 1:2,000,000. Dept. Mines Geol, Kathmandu.

Ni, J.F., Guzman-Speziale, M., Bevis, M., Holt, W.E., et al., 1989. Accretionary tectonics of Burma and the three-dimensional geometry of the Burma subduction zone. Geology 17, 68–71.

Pandey, M.R., Tandukar, R.P., Avouac, J.P., Lavé, J., Massot, J.P., 1995. Interseismic strain accumulation on the Himalayan crustal ramp (Nepal). Geophys. Res. Lett. 22, 751–754.

Rubin, C.M., Sieh, K., Chen, Y.-G., Lee, J.-C., et al., 2001. Surface rupture and behavior of thrust faults probed in Taiwan. EOS Trans. Am. Geophys. Union 82, 565–569.

Seno, T., Stein, S., Gripp, A.E., 1993. A model for the motion of the Philippine Sea Plate consistent with NUVEL-1 and geological data. J. Geophys. Res. 98, 17941–17948.

Shin, T.C., Kuo, K.W., Lee, W.H.K., Teng, T.L., Tsai, Y.B., 2000. A preliminary report of the 1999 Chi-Chi (Taiwan) earthquake. Seismol. Res. Lett. 71, 24–30.

Suppe, J., 1981. Mechanics of mountain building and metamorphism in Taiwan. Mem. Geol. Soc. China 4, 67–89.

Suppe, J., 1984. Kinematics of arc–continent collision, flipping of subduction, and back-arc spreading near Taiwan. Mem. Geol. Soc. China 6, 21–33.

Suppe, J., 1988. Tectonics of arc–continent collision on both sides of the South China Sea: Taiwan and Mindoro. Acta Geol. Taiwanica 26, 1–18.

Suppe, J., Chang, Y.-L., 1983. Kink method applied to structural interpretation of seismic sections, western Taiwan. Pet. Geol. Taiwan 19, 29–49.

Taymaz, T., Jackson, J., Westaway, R., 1990. Earthquake mechanisms in the Hellenic trench near Crete. Geophys. J. Int. 102, 695–731.

Toksoz, M.N. (Ed.), 2002. Special Issue: The Izmit, Turkey, earthquake of 17 August 1999. Bull. Seismol. Soc. Am., vol. 92, pp. 1–526.

Wu, F.T., Rau, R.-J., Salzberg, D., 1997. Taiwan orogeny: thin-skinned or lithospheric collision? Tectonophysics 274, 191–220.

Wu, F.T., Chang, C.S., Wu, Y.M., 2003. Precisely relocated hypocenters, focal mechanisms and active orogeny in central Taiwan. J. Geol. (submitted for publication).

Yang, K.-M., Ting, H.-H., Yuan, J., 1991. Structural styles and tectonic modes of Neogene extensional tectonics in southwestern Taiwan: implications for hydrocarbon exploration. Pet. Geol. Taiwan 26, 1–31.

Yeats, R.S., Sieh, K., Allen, C.R., 1997. The Geology of Earthquakes. Oxford Univ. Press, New York.

Yeh, M.-G., Yang, C.-Y., 1994. Depositional environment of the upper Miocene to Pleistocene series in the Chungpu area, Chiayi, Taiwan. Pet. Geol. Taiwan 29, 193–224.

Yin, A., Harrison, T.M., 2000. Geologic evolution of the Himalayan–Tibetan orogen. Annu. Rev. Earth Planet. Sci. 28, 211–280.

Yu, S.-B., Chen, H.-Y., Kuo, L.-C., 1997. Velocity field of GPS stations in the Taiwan area. Tectonophysics 274, 41–59.

Zhao, W., Nelson, K.D., and Project INDEPTH Team, 1993. Deep seismic reflection evidence for continental underthrusting beneath southern Tibet. Nature 366, 557–559.